Indian Journal of Chemistry
Vol. 62, October 2023, pp. 1040-1046
DOI: 10.56042/ijc.v62i10.6181

Theoretical investigation of BODIPY based compounds as photosensitizers in photodynamic therapy

Buthaina Kamel[a], Wesam Bachir[a,b] & Moustafa Sayem El-Daher*[a,c]

[a] Higher Institute for Laser Research and Applications, Damascus University, Syria

[b] Institute of Metrology and Biomedical Engineering, Faculty of Mechatronics, Warsaw University of Technology, Św. A. Boboli 8 St., 02-525 Warsaw, Poland

[c] Arab International University, Daraa, Syria

E-mail: m.saemaldaher@damascusuniversity.edu.sy, eldaherm@gmail.com

Received 1 October 2022; accepted (revised) 18 August 2023

In this work we carried out theoretical evaluation of the potential use of BODIPY and related compounds as photosensitizer in photodynamic therapy (PDT). Five compounds bearing the chromophore of 4,4-difluoro-4-bora-3a,4a-diaza-s-indacene (BODIPY) with substituent elements from the fourth column in the periodic table (Si-Ge-Sn-Pb) have been investigated. In the present study the density functional theory and its time dependent extension TD-DFT have been used to calculate the energy of ground, singlet-triplet excited states and energy for $\left(\Delta E_{S_o} - s_1, \Delta E_{S_o} - T_2\right)$ The electronic absorption spectra, transition dipole moments (TDM) for spin-allowed $S_0 \rightarrow S_n$ and other properties have been calculated. The results of this work show that among the studied compounds, PM-Sn is potentially the best option for photosensitizer in PDT.

Keywords: TD-DFT, PDT, BODIPY, Photosenstizers, TDM, Electronic absorption spectra

Photodynamic therapy (PDT) has a potential for non-invasive treatment of both neoplastic and non-neoplastic tumors[1]. PDT includes three main elements: light, photosensitizer PS and oxygen. Any of these components is not toxic by itself, but together all these components initiate the production of cytotoxic agents inducing cell death[2].

When light is absorbed, the photosensitizer is transferred from its singlet ground state to an unstable excited singlet state (1PS*) through a process of intersystem crossing (ISC)[3]. The photosensitizer in the excited singlet state can spin-flip into the excited triplet state (3PS*). Mainly there are two mechanisms included in the photodynamic reaction(type I, type II). In type I the activated 3PS* reacts directly with a biological substrate *via* electron or hydrogen transfer, producing free radical species, these species can further react with molecular oxygen ($3O_2$), generating the reactive oxygen species (ROS). In type II, the activated 3PS* transforms its excitation energy directly to molecular oxygen, producing the highly reactive singlet oxygen ($1O_2$)[4]. The ratio between these two mechanisms depends on the type of the PS used, as well as the concentrations of substrate and oxygen[5].The reactive oxygen species targets cell membranes causing damage to the cell, in studying photosentizers two aspects are taken in to consideration, First the allocation and localization of photosentizers in the biological cells. Second their photo-physical abilities to generate reactive oxygen species. Earlier theoretical studies often focused on these aspects and overlooked the first one. This is because handling the two aspects requires different methodology[6,7]. Generating singlet oxygen using a photosensitizer is related to the existence of a singlet–triplet gap $\Delta E_{S_o} - T_1$ higher than 0.98v and having absorption light in the near IR range to ensure deep penetration of the tissues[8,9]. PSs are usually either porphyrin or non-porphyrin based. A good PDT photosensitizer is expected to have High selectivity toward cancer cells, high triplet state yields and long triplet state lifetimes and able to produce toxic reactive oxygen species (*e.g.*, $1O_2$) or free radicals, Near IR light absorption and absence of dark toxicity[10,11]. Up to date, no photosensitizer could satisfy all of the mentioned requirements. Therefore, many wide ranging studies were carried out aiming to design new PSs with better properties for PDT. (4,4-Difluoro-4-bora-3a,4a-diaza-s-indacene) -or shortly BODIPY dyes-are very important class of

organic fluorophores, used for diverse applications such as an artificial sensitizers for solar cells, molecular photonic wires, sensors and light-harvesting materials, labels and imaging probes[12,13]. In addition to photodynamic therapy[14], applications of these dyes go well beyond classical sensing and imaging, they include photothermal and photodynamictumor therapy, photoacoustic imaging and energy conversion. In optical *p*H sensing[15,16], BODIPY is considered a new non-porphyrinic class of PS and offers a number of attributes that might attract photodynamic applications, including synthetic tunability of their absorption features, chemical robustness with high extinction coefficients and negligible photo bleaching[17]. Because of the living tissue's therapeutic window (500–800 nm), photosensitizers are generally designed to absorb red light. However, light with a shorter wavelength can be used when tissue penetration is not important. One interesting major factor about BODIPY dyes is the absorption and emission characteristics which can be tuned by introducing appropriate substituents to BODIPY. The substitution affects energy of the HOMO-LUMO orbitals, and the population of the triplet state thus influences the phenomena of absorption which is of importance in photodynamic therapy (PDT)[18-20].

DFT especially on the level of TD-DFT is considered powerful tools for theoretically predicting the spectroscopic properties of large molecular systems. Special attention should be paid to the choice of the approximated exchange-correlation functional which affects the accuracy of the results[21,22].

Recently, there were many theoretical and experimental results reported on BODIBY as a promising chemical structure for making new derivatives to be used as a photosensitizers in photodynamic therapy with improved features when applied clinically[23,24].Modifying the structure by introducing heavy atoms in the BODIPY core or connect BODIPY core to other molecules[25] could help improve the desired properties.

In this work, we theoretically explore the effects of the substitution of atoms from the fifth column in the periodic table in the BODIPY core on the absorption wavelength and singlet-triplet energy gap. This enables us to predict the change in photo physical properties of BODIPY resulting from introducing an atom (Si-Ge-Sn-Pb) in the BODIPY core and based on theoretical results we can suggest novel molecular systems derived from BODIPY suitable for use as photosensitizers in PDT which can improve the application of PDT in future treatments.

Computational details

Theoretical calculation of the ground state was carried out using DFT, while the excited singlet and triplet states were calculated using TD-DFT. The functional used in the calculations was (B3LYP) with a basis set (6-31G, LanL2DZ). Geometry optimizations performed in the gas phase and in a Polarizable Continuum Model (shortly PCM) of solvents[26,27]. All DFT and TD-DFT calculations were carried out using Gaussian 09 software package[28]. The molecules shown in the Fig. 1 and Table 1 have been studied. Where the carbon atom at the site 6 was replaced by atoms Si, Ge, Sn, Pb.

Results and Discussion

Geometry

The ground state structural parameters of BODIPY and the studied compounds obtained from DFT/ B3LYP/6-31G (lanl2d for Sn and Pb) calculations. The resulting Bond length, Bond angles and Dihedral angles are presented in Table 2. The biggest increase in the bond length C5-C6 happened when substitution with Pb in (C5-Pb6) and biggest increase in the bond length C1-C6 happened when substitution with Pb in (C1-Pb6). With regard to the bond angles, the smallest value when location 6th was replaced with Pb, while for Dihedral angles showed biggest value change when Pb is used.

As shown in the Fig. 2, The electron density difference maps which shows electronic density in position 6 in case of C,Si and do not show this density

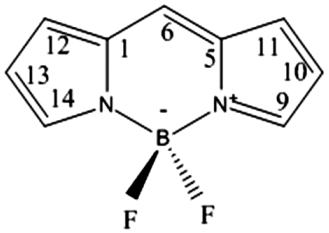

Fig. 1 — Molecular structure of the BODIPY dye and the related compounds

Table 1 — The five molecules studied in this work

Molecule	I	II	III	VI	V
PM-6	PM-C	PM-Si	PM-Ge	PM-Sn	PM-Pb

Table 2 — Bond length [Å], Bond angles [°], Dihedral angles [°] for PM for ground state

	Atoms	Calculated	Atoms	Calculated
PM-C	C(5)-C(6)	1.3924	C(5)-C(6)-C(1)	121.7616
	N(4)-C(9)	1.3519	C(6)-C(5)-N(4)	120.4047
	N(4)-C(5)	1.4084	C(5)-N(4)-B(3)	125.4343
	C(1)-C(6)	1.3924	F(8)-B(3)-F(7)	109.6157
	B(3)-F(7)	1.4253	N(4)-B(3)-N(2)	106.5603
	B(3)-N(4)	1.5569	B(3)-N(2)-C(1)	125.4343
	N(2)-C(14)	1.3519	C(6)-C(1)-N(2)	120.4047
PM-Si	C(5)-Si(6)	1.7793	C(5)-Si(6)-C(1)	110.7442
	N(4)-C(9)	1.3633	Si(6)-C(5)-N(4)	117.5108
	N(4)-C(5)	1.4184	C(5)-N(4)-B(3)	127.1565
	C(1)-Si(6)	1.7793	F(8)-B(3)-F(7)	109.4535
	B(3)-F(7)	1.4442	N(4)-B(3)-N(2)	112.0694
	B(3)-N(4)	1.5553	B(3)-N(2)-C(1)	127.1385
	N(2)-C(14)	1.3633	Si(6)-C(1)-N(2)	117.5187
PM-Ge	C(5)-Si(6)	1.7793	C(5)-Ge(6)-C(1)	109.0844
	N(4)-C(9)	1.3633	Ge(6)-C(5)-N(4)	116.7338
	N(4)-C(5)	1.4184	C(5)-N(4)-B(3)	127.4215
	C(1)-Si(6)	1.7793	F(8)-B(3)-F(7)	109.6724
	B(3)-F(7)	1.4442	N(4)-B(3)-N(2)	112.6607
	B(3)-N(4)	1.5553	B(3)-N(2)-C(1)	127.4096
	N(2)-C(14)	1.3633	Ge(6)-C(1)-N(2)	116.7702
PM-Sn	C(5)-Sn(6)	2.0199	C(5)-Sn(6)-C(1)	104.7837
	N(4)-C(9)	1.3697	Sn(6)-C(5)-N(4)	115.2706
	N(4)-C(5)	1.4178	C(5)-N(4)-B(3)	126.9764
	C(1)-Sn(6)	2.0198	F(8)-B(3)-F(7)	110.6957
	B(3)-F(7)	1.448	N(4)-B(3)-N(2)	113.7445
	B(3)-N(4)	1.5574	B(3)-N(2)-C(1)	126.9727
	N(2)-C(14)	1.3698	Sn(6)-C(1)-N(2)	115.2703
PM-Pb	C(5)-Pb(6)	2.0635	C(5)-Pb(6)-C(1)	103.3416
	N(4)-C(9)	1.3725	Pb(6)-C(5)-N(4)	115.0432
	N(4)-C(5)	1.4136	C(5)-N(4)-B(3)	126.8777
	C(1)-Pb(6)	2.0634	F(8)-B(3)-F(7)	110.984
	B(3)-F(7)	1.4487	N(4)-B(3)-N(2)	113.7441
	B(3)-N(4)	1.5568	B(3)-N(2)-C(1)	126.866
	N(2)-C(14)	1.3726	pb(6)-C(1)-N(2)	115.0465
	Atoms		Calculated (exp) [16]	
PM-C	C(1)-C(12)-C(13)-C(14)		-0.0000 (-0.0)	
	C(14)-N(2)-B(3)-N(4)		179.9985 (179.5)	
PM-Si	N(2)-C(1)-Si(6)-C(5)		3.4573	
	B(3)-N(4)-C(5)-C(11)		170.o431	
PM-Ge	N(2)-C(1)-Ge(6)-C(5)		4.5754	
	B(3)-N(4)-C(5)-C(11)		169.1548	
PM-Sn	N(2)-C(1)- Sn(6)-C(5)		7.6741	
	B(3)-N(4)-C(5)-C(11)		167.7182	
PM-Pb	N(2)-C(1)-Pb (6)-C(5)		9.3110	
	B(3)-N(4)-C(5)-C(11)		167.7663	

in case of Pb, Sn and Ge while Table 3, Table 4 and Table 5 show calculations for oscillator strengths (*f*) and transition dipole moments (TDM) of the spin-allowed $S_0 \rightarrow S_n$in Acetonitrile, Ethanol and DMSO solutions.

Absorption

In PDT it's important that the absorption wave length is within the infrared spectral range. We list the calculated absorption properties of the molecules studied using TD-DFT using a number of solvents and including transition of HOMO →LUMO oscillator strengths.

The results listed in Table 3, Table 4 and Table 5 show that the absorption wavelengths of the five studied compounds did not significantly change by replacing the solution by Ethanol, DMSO or acetonitrile. The change was (1, 18, 13, 29, 8.43) nm for the compounds (PM-C, PM-Si, PM-Ge, PM-Sn, PM-Pb) respectively. The type of solventdid not impact the transition $S_0 \rightarrow S_n$for the studied compounds when studied with different solutions. PM-Sn had the biggest shift which is 29nm. However replacing the carbon atom at position 6 with (Si, Ge, Sn and Pb) significantly red-shifts the absorption wavelengths in the compound. Each replacement has a different redshift in the solution as follow: Ethanol solution: replacing the carbon with (Si, Ge, Sn and Pb) causes redshifts of (124.83, 139.44, 175.04 and 464.77nm) causing the absorption wavelengths to become (546.27, 560.88, 669.48 and 886.21nm) respectively. DMSO solution: replacing the carbon with (Si, Ge, Sn and Pb) causes red shifts of (141.89, 137.09, 268.4 and 454.96nm) and the absorption wavelengths become (564.80, 560, 669.48, 877.97 nm) respectively. In Acetonitrile solution replacing the carbon with (Si, Ge, Sn and Pb) causes red shifts about (140.59, 125.47, 277.65 and464.77nm) respectively and the absorption wavelengths to become (562.03, 546.61, 698.65 and 886.21nm) respectively.

There are many molecular orbital pairs involved in each $S_0 \rightarrow S_n$ transition, however, only those with higher probability of occurrence are provided in Table 3, Table 4 and Table 5. In ethanol as shown in Table 3. The TDMs of $S_0 \rightarrow S_2$ in PM-Si was (dx=dy=dz=0.0) and $S_0 \rightarrow S_3$ (dx=dz=0, dy=0.2) (Table 4). The same values were observed for PM-Si in DMSO (Table 5), while in acetonitrile the TDMs of $S_0 \rightarrow S_1$ in PM-Si was (dx=1.8, Dy= dz= 0.0). Atomic contributions are shown in Fig. 3.

Triplet energy

It is important in PDT, that the triplet state has enough energy to generate singlet oxygen in addition to the deeper penetration of tissues, that's why we list in Table 6 the excitation energies of the studied compounds in a number of solvent calculated using TD-DFT.

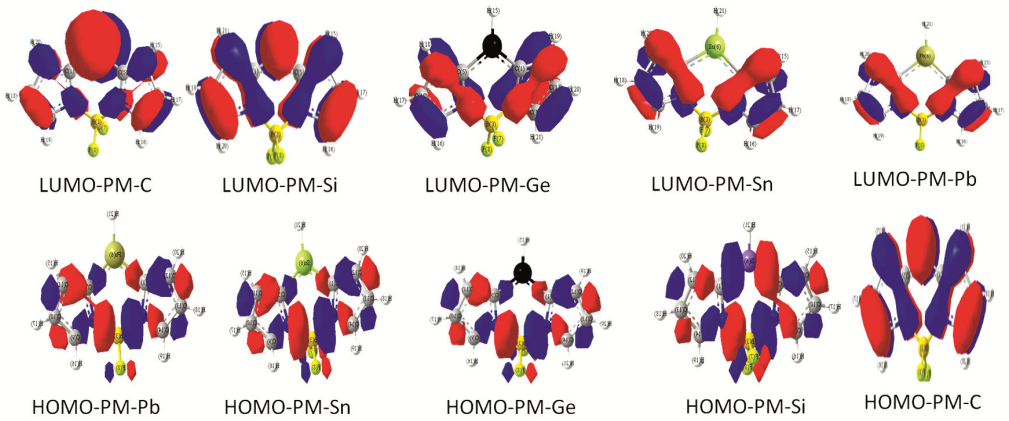

Fig. 2 — HOMO and LUMO states for all studied compounds

Table 3 — The parameters of the transition dipole moments (TDM) for spin-allowed $S_0 \rightarrow S_n$, oscillator strengths (f).TD-DFT/B3LYP/ PCM/6-31G (LanL2DZ for Sn-Pb) in Ethanol solution

Ethanol	$S_0 \rightarrow S_n$	TDM [a.u]				MO	λ [nm] ([eV])	f [a.u.]
		dx	dy	dz	Dip			
PM-C	→S1	2.2	0.2	-0.0	4.9	H-0→L+0 (91%)	421.44(2.94)	0.2917
	→S2	0.4	0.2	0.0	0.2	H-1→L+0 (90%)	369.28(3.35)	0.0170
	→S3	0.3	0.3	-0.3	0.3	H-2→L+0 (96%)	293.98(4.21)	0.0327
PM-Si	→S1	-1,9	0,4	-0,0	3,9	H-0→L+0 (99%)	546.47(2,19)	0.2144
	→S2	0,0	-0,0	-0,0	0,0	H-0→L+1 (80%)	417.67(2. 96)	0.0006
	→S3	-0,0	0,2	0,0	0,0	H-2→L+0 (82%)	413.03(3.00)	0.0039
PM-Ge	→S1	1,8	-0,0	0,1	3,4	H-0→L+0 (98%)	560.88(2.21)	0.1872
	→S2	0,1	-0,1	-0,0	0,0	H-1→L+0 (97%)	470.92(2.63)	0,0030
	→S3	0.7	-1,4	-0,1	2,6	H-2→L+0 (92%)	361.35(3.43)	0.2187
PM-Sn	→S1	1,6	-1,6	0,0	2,9	H-0→L+0 (98%)	696.48(1.68)	0.2307
	→S2	0,4	0,1	0,0	0,1	H-2→L+0 (94%)	501.58(2.47)	0.0177
	→S3	-0,1	1,0	0,2	1,1	H-1→L+0 (86%)	452.93(2.72)	0.1121
PM-Pb	→S1	0.9	-1	0,0	1.9	H-0→L+0 (98%)	886.21(1.39)	0.0671
	→S2	0.4	0.4	0,0	0.4	H-2→L+0 (70%)	579.81(2.13)	0,0233
	→S3	-0.5	-1,2	-1,1	1,7	H-1→L+0 (68%)	561.50(2.20)	0.0970

Table 4 — The parameters of the transition dipole moments (TDM) for spin-allowed $S_0 \rightarrow S_n$, oscillator strengths (f).TD-DFT/B3LYP/ PCM/6-31G (LanL2DZ for Sn-Pb) in DMSO solution

DMSO	$S_0 \rightarrow S_n$					MO	λ [nm] ([eV])	f [a.u.]
		Dx	dy	dz	Dip			
PM-C	→S1	2.4	0.0	0.1	5.8	H-0→L+0 (92%)	422.91(2.93)	0.4178
	→S2	-1.1	0.3	0.0	1.4	H-1→L+0 (91%)	368.99(3.36)	0.1179
	→S3	-0.5	-0.6	0.0	0.7	H-2→L+0 (96%)	294.06(4.21)	0.0797
PM-Si	→S1	-1,9	0,4	-0,0	4,0	H-0→L+0 (99%)	564.80(2.19)	0.2195
	→S2	0,0	-0,0	-0,0	0,0	H-0→L+1 (86%)	417.30(2.97)	0.0006
	→S3	-0,0	-0,2	0,0	0,0	H-2→L+0 (88%)	411.62(3.01)	0.0041
PM-Ge	→S1	-1,8	0.0	-0.1	3,5	H-0→L+0 (98%)	560.00(2.21)	0.1915
	→S2	0,1	-0.1	-0.0	0,0	H-1→L+0 (97%)	467.95(2.64)	0.0030
	→S3	0.7	-1.4	-0.1	2,6	H-2→L+0 (92%)	362.12(3.42)	0.2243
PM-Sn	→S1	1,7	-0.1	0.0	2,9	H-0→L+0 (98%)	690.75(1.79)	0.2356
	→S2	0.4	0.1	-0.0	0.2	H-2→L+0 (94%)	497.34(2.49)	0.0183
	→S3	-0.1	1.0	0.2	1.2	H-1→L+0 (87%)	450.81(2.49)	0.1184
PM-Pb	→S1	0.9	-1.0	0.0	1,9	H-0→L+0 (`97%)	877.87(1.41)	0.0690
	→S2	0.5	0.7	0, 1	0.8	H-2→L+0 (50%)	575.89(2.15)	0.0448
	→S3	-0.4	-1.1	-0.1	1.4	H-1→L+0 (49%)	559.27(2.21)	0.0781

Table 5 — the parameters of the transition dipole moments (TDM) for spin-allowed S0→Sn, oscillator strengths (f).TD-DFT/B3LYP/PCM/6-31G (LanL2DZ for Sn-Pb) in acetonitrile solution

Acetonitrile	S0→Sn	TDM [a.u]				MO	λ [nm] ([eV])	f [a.u.]
		Dx	dy	Dz	Dip			
PM-C	→S1	2.3	0.0	0.1	5.5	H-0→L+0 (91%)	420.72(2.94)	0.4009
	→S2	-1.1	0.3	0.0	1.4	H-1→L+0 (90%)	368.71(3.36)	0.1222
	→S3	-0.5	-0.6	0.0	0.7	H-2→L+0 (95%)	293.85(4.21)	0.0778
PM-Si	→S1	1.8	0.0	0.0	3.5	H-0→L+0 (71%)	562.03(2.20)	0.2259
	→S2	-1.7	0.3	-0.0	3.1	H-1→L+0 ((70%)	413.39(2.99)	0.0008
	→S3	-0.5	-0.2	0.1	0.4	H-3→L+0 (64%)	409.59(3.02)	0.0049
PM-Ge	→S1	2.1	0.0	-0.0	4.8	H-0→L+0 (39%)	546.91(2.26)	0.3002
	→S2	1.4	-0.2	-0.0	2.1	H-1→L+0 (77%)	449.79(2.75)	0.1459
	→S3	-0.2	-0.2	0.0	0.1	H-2→L+0 (92%)	362.54(3.42)	0.0114
PM-Sn	→S1	2.2	0.2	-0.0	4.9	H-0→L+0 (98%)	698.65(1.77)	0.2894
	→S2	0.4	0.2	0.0	0.2	H-1→L+0 (97%)	449.79(2.75)	0.0170
	→S3	0.3	0.3	-0.3	0.3	H-3→L+0 (52%)	362.54(3.42)	0.0321
PM-Pb	→S1	1.9	-0.7	0.0	4.2	H-0→L+0 (99%)	886.21(1.39)	0.2264
	→S2	0.5	0.6	-0.0	0.6	H-1→L+0 (32%)	579.81(2.13)	0.0442
	→S3	-0.3	0.5	0.0	0.4	H-2→L+0 (66%)	561.50(2.08)	0.0306

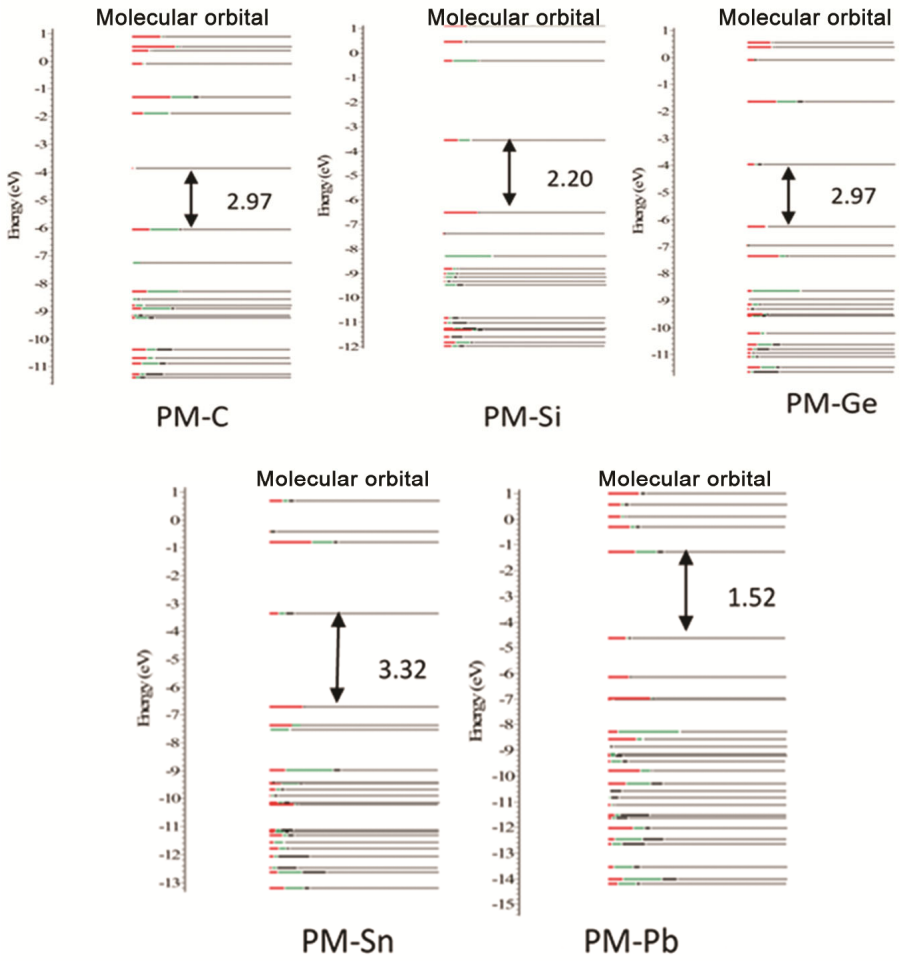

Fig. 3 — Molecular orbital energy levels [eV] with contributions from (C,Si,Ge,Sn,Pb) (red), N (green) and B(black) atoms as well as energy gap values (Egap) [eV] for PM-C, PM-Si,PM-Ge, PM-Sn,PM-Pb

Table 6 — Vertical excitation energies [eV] to the lowest singlet and triplet excited states by TD-DFT/B3LYP/ /6-31G (LanL2DZ for Ge- Sn-Pb) in Ethanol, acetonitrile, and DMSO solution

PM		PM-C	PM-Si	PM-Ge	PM-Sn	PM-Pb
gas phase	$\Delta E_{S_0-S_1}$	2.90	2.08	2.03	1.55	1.22
	$\Delta E_{S_0-S_1}$	1.50	0.49	0.91	2.11	0.006
Ethanol	$\Delta E_{S_0-S_1}$	2.94	2.19	2.21	1.78	1.39
	$\Delta E_{S_0-S_1}$	1,57	0.75	0.75	1.09	0.71
acetonitrile	$\Delta E_{S_0-S_1}$	2.94	2.20	2.26	1.77	1.39
	$\Delta E_{S_0-S_1}$	1.56	0.75	1.11	1.11	1.41
DMSO	$\Delta E_{S_0-S_1}$	2.93	2.19	2.21	1.79	1.41
	$\Delta E_{S_0-S_1}$	1.56	0.76	1.12	0.76	0.74

For efficiency in PDT, the first excited singlet state for photosensitizer must be triggered with an energy between 1.55ev (1800nm) and 1.77ev (700nm), this range of energy gives deeper penetration into tissues. In addition there should be enough triplet energies higher than0.98ev.Among the studied compounds, the PM-Sn has this kind of attributes, because its state $\left(\Delta E_{s_o}-T_1\right)$ is attained with a photon whose energy is 1.77ev (698.65nm) in the acetonitrile solution. This leads to state T_1 with energy1.11ev, also PM-Sn shows the same behavior in the Ethanol solution, because the state S_1 takes a place with a photon whose energy is 1.68ev(696.48 nm), this leads to state T_1 with energy 1.09ev, but the PM-Sn within the DMSO solution shows triplet state energy not enough to produce the singlet oxygen(0.76ev).

In case of PM-Ge compound, we noticed the absence of absorption lines inside the required spectral range, the triplet state energy in Ethanol solution (0.75ev) is not enough to produce the singlet oxygen, but in acetonitrile and DMSO in which it takes the values (1.11, 1.12ev)respectively, it is enough to produce the singlet oxygen. In the PM-Pb, we found that the low triplet state energy in the Ethanol and DMSO solutions (0.74,0.71 ev), but at the same time this energy in acetonitrile solution raises up to (1.41)which is enough to produce the singlet oxygen.

Finally in PM-Si, the triplet state energy in all the solutions is lower than the threshold energy to yield singlet oxygen (0.75, 0.75, 0.76ev). Consequently, they are not considered an effective photosensitizers in PDT.

Conclusion

In this work, we studied the physical properties of 4,4-Difluoro-4-bora-3a,4a-diaza-s-indacene (BODIPY) and we replaced carbon in position 6 with elements from the fourth column of the periodic table (Si, Ge, Sn and Pb). DFT method was used for ground state and TD-DFT for excited states associated with the C-PCM model. We have calculated the absorption wavelength and energy gaps between the first triplet energy and ground state energy $\left(\Delta E_{s_o}-T_1\right)$ together with different solutions (Ethanol, Acetonitrile and DMSO) because of their influence on the properties important for photodynamic therapy. The results can be summarized as follows:

The replacement in position 6 with elements (Si, Ge, Sn and Pb) gave Q-bands peaks higher than 500nm. The highest Q-Band peak has been found in the PM-Pb in all solutions.

The lowest energy for producing singlet oxygen was found in PM-Ge and PM-Pb both in Ethanol solution, and in PM-Si in all solutions.

Based on the two previous properties, we conclude that PM-Sn is potentially a very good photosensitizer for photodynamic therapy. Future work should include experimental studies to validate the theoretical results and for synthesizing, promising compounds to be used in photodynamic therapy.

Acknowledgments

The Authors would like to thank Dr. Omar Bobes (Physikalisches Institut Georg-August-University of Goettingen) for his support and for helping in theoretical calculations using Gaussian 09 software.

References

1 Gunaydin G, Gedik M E & Ayan S, *Frontiers Chem*, 9 (2021) 1.

2 Kubrak T, Karakuła M, Czop M, Kawczyk-Krupka A & Aebisher D, *Molecules*, 27 (2022) 1.

3 Hao B, Wang J, Wang C, Xue K, Xiao M, Lv S & Zhu C, *Chem Sci*, 13 (2022) 4139.
4 Sai D L, Lee J, Nguyen D L & Kim Y P, *Exp Mol Med*, 53 (2021) 495.
5 Zhang Z J, Wang K P, Mo J G, Xiong L & Wen Y, *World J Stem Cells*, 12 (2020) 562.
6 Pederzoli M, Baig M W, Kyvala M, Pittner J & Cwiklik L, *J Chem Theory Comp*, 15 (2019) 5046.
7 Liu M, Chen Y, Guo Y, Yuan H, Cui T, Yao S, Jin S, Fan H, Wang C, Xie R, He W & Guo Z, *Nat Commun*, 13 (2022) 1. (https://doi.org/10.1038/s41467-022-29872-7).
8 Momeni M R & Brown A, *J Phy Chem A*, 120 (2016) 2550.
9 Nguyen V N, Yan Y, Zhao J & Yoon J, *Acc Chem Res*, 54 (2021) 207.
10 Kustov A V, Morshnev P K, Kukushkina N V, Smirnova N L, Berezin D B, Karimov D R, Shukhto O V, Kustova T V, Belykh D V, Mal'shakova M V, Zorin V P & Zorin T E, 23 (2022) 5294. (https://doi.org/10.3390/ijms23105294).
11 Wu Y, Li S, Chen Y, He W & Guo Z, Chem Sci, 13 (2022) 5085.
12 Scholz M, Hoffmann C, Klein J R, Wirtz M, Jung G & Oum K, *Zeitschrift für Physikalische Chemie*, 234 (2019) (https://doi.org/10.1515/zpch-2019-1374).
13 Madrid-Úsuga D, Ortiz A & Reina J H, *ACS Omega*, 7 (2022) 3963.
14 Prieto-Montero R, Prieto-Castañeda A, Sola-Llano R, Agarrabeitia A R, García-Fresnadillo D, López-Arbeloa I, Villanueva A, Ortiz M J, Moya S D L & Martínez-Martínez V, *Photochem Photobiol*, 96 (2020) 458.
15 Staudinger C, Breininger J, Klimant I & Borisov S M, *Analyst*, 144 (2019) 2393.
16 Merkes J M, Lammers T, Kancherla R, Rueping M, Kiessling F & Banala S, *Adv Opt Mater*, 8, (2020) 1902115, (https://doi.org/10.1002/adom.201902115).
17 Zhang W, Ahmed A, Cong H, Wang S, Shen Y & Yu B, *Dye Pigment*, 185 (2021) 108937.
18 Awuah S G & You Y, *RSC Adv*, 2 (2012) 11169.
19 Fan Y, Zhang J, Hong Z, Qiu H, Li Y & Yin S, *Polymers* (*Basel*), 13 (2021) 75.
20 Alkhatib Q, Helal W & Marashdeh A, *RSC Adv*, 12 (2022) 1704.
21 Drzewiecka-Matuszek A & Rutkowska-Zbik D, *Molecules*, 26 (2021) 7176.
22 Aslanoglu B, Yakavets I, Zorin V, Lassalle H P, Ingrosso F, Monari A & Catak S, *Phys Chem Chem Phys*, 22 (2020) 16956.
23 Simone B C D, Mazzone G, Sang-Aroon W, Marino T, Russo N & Sicilia E, *Phys Chem Chem Phys*, 21 (2019) 3446.
24 Ponte F, Mazzone G, Russo N & Sicilia E, *J Mol Mode*, 24 (2018) 1 (https://doi.org/10.1007/s00894-018-3727-3)
25 Ponte F, Alberto M E, De Simone BC, Russo N & Sicilia E, *Inorg Chem*, 58 (2019) 9882.
26 Wang J & Durbeej B, *J Comp Chem*, 41, (2020) 1718.
27 Herbert J M, *Wiley Interdiscip Rev Comp Mol Sci*, 11 (2021), (https://doi.org/10.1002/wcms.1519).
28 Barone V, Bloino J & Biczysko M, Vibrationally-resolved electronic spectra in GAUSSIAN 09. Revision A, 2 (2009) 1-20.